

ISSN: 2349-5162 | ESTD Year : 2014 | Monthly Issue JOURNAL OF EMERGING TECHNOLOGIES AND INNOVATIVE RESEARCH (JETIR)

An International Scholarly Open Access, Peer-reviewed, Refereed Journal

Anticancer Potential of Biocompatible Oxime Esters; Synthesis, anticancer, antibacterial, DNA binding, DNA photocleavage and molecular docking studies

P. J. Bindu^{a*}, T. R. Ravikumar Naik^b, S. Chandrashekar^{a,c}

^aDepartment of Chemistry, A. S. M. Women's College, Ballari, Karnataka-583 104, India ^bDepartment of P. G. Studies in Chemistry, Veerashaiva College, Ballari, Karnataka -583 104, India ^cDepartment of Organic Chemistry, Indian Institute of Science, Bangalore 560 012, India.

Abstract

A series of substituted oxime esters have been synthesized and tested for their anticancer, antibacterial, DNA photocleavage and molecular docking studies. The in-house synthesized oxime esters were characterized by IR, ¹H NMR, and mass spectra. Most of oxime esters showed good antibacterial and anticancer activity. All these compounds were found to cleave DNA upon irradiation with 365 nm UV light. The results indicated that oxime esters underwent homolysis of their weak N-O bonds on direct and photosensitized UV photolysis to afford iminyl and carboxy radicals which can then cause the cleavage of the pUC 19 DNA. A plausible reaction mechanism is also proposed. The interaction of between DNA protein with oxime esters was also evaluated by CT-DNA binding and molecular docking studies.

Keywords: Oxime esters, Antibacterial, Anticancer, DNA photocleavage, DNA binding, Molecular docking.

1. INTRODUCTION

The understanding and quantification of DNA-ligand interactions [1,2], are of paramount importance for the study of biological mechanisms and for many applications such as drug design. Intercalation by stacking of smaller aromatic ligand moieties between the nucleobases plays a significant role in a multitude of DNA interactions [3]. There have been however; relatively few consistent experimental studies on the parent association energies and their dependence on ligand structure until now. Small molecules can interact with DNA in non-covalent fashion and in most important applications it is by an intercalative mode. Generally the intercalative molecules should contain an extended heteroatom, as its stacking between base pairs is considered to be a major driving force that leads to binding [4]. The binding mode and strength are sensitively dependent on the shape, planar area, size and electron density of the interacting aromatic rings. So a systematic study on the influence of varying parameters on the

* Corresponding author. Tel.: ++91-99007-92675; e-mail: naikravi7@gmail.com

interaction of small molecules with DNA would be valuable in the rational design of new drugs and therapeutic reagents targeted to DNA [5-10].

The compounds with efficient photo-induced DNA cleavage activity are of increasing importance in nucleic acid chemistry and medicinal applications based on the photodynamic therapy (PDT) for cancer [11-14]. To achieve significant photocytotoxic effect, most modern PDT applications involve three key components: a photosensitizer, a light source and tissue oxygen [15-17]. The procedure requires exposure of tissues to a photosensitizing drug followed by irradiation with visible light of the appropriate wavelength, usually in the red or near-infrared region and compatible with the absorption spectrum of the drug. Upon absorption of a photon, the photosensitizer undergoes one or more energy transitions and usually emerges in its excited triplet state. The triplet state can participate in a one-electron oxidation–reduction reaction (type I photochemistry) with a neighboring molecule, producing free radical intermediates that can react with oxygen to produce peroxy radicals and various reactive oxygen species (ROS) [15-17].

Molecular docking has been a focus of attention for many years. In the current scenario, the flexible docking program is able to predict protein ligand complex structures with reasonable accuracy and speed [18]. There has been very little application of docking studies to interpretation of the DNA binding affinity, in modern chemistry and biochemistry. To obtain a significant correlation, it is essential that appropriate descriptors are employed, whether they are theoretical, empirical or derived from readily available experimental characteristics of structures. Many descriptors reflect simple molecular properties and can thus provide insight into the physicochemical nature of the activity/property under consideration [12]. Subsequently, several researchers have reported correlations for a wide variety of chemical properties such as including DNA binding studies [19,20].

Further, oxime esters functional group systems are an important class of nitrogen-oxygen hetero junction with many synthetic applications as functional units of many molecules of biological interest that has made them useful intermediates in medicinal chemistry [21]. Due to their biological activities, they have been the subject of extensive experimental studies [22-26], and many synthetic methods have been employed in the synthesis [27-29]. The advantages of oxime esters include their ease of handling and characterization in comparison with peroxides or azo-compounds, and therefore further investigation of the scope and limitations of their free radical chemistry was an attractive prospect [30,31].

Fig.1. Biologically important oxime esters.

Recently, Walton, explained that, the functionalized oximes as efficient precursor materials for the generation of carbon-, nitrogen- and oxygen-centered radicals for novel biological activities [32]. In this context, oximes appear quite attractive due to their relative biological versatility. The oxime esters, being appeared in

several known anticancer or DNA photocleaver (Fig.1) [33], has been angularly fused to the aromatic skeleton. The introduction of methoxy group and similar analogues commonly applied in anticancer drugs, were incorporated into the parent structure not only to increase the affinity with DNA but also to elucidate the influence of them on biological activities [33].

In recent years much interest has been focused on design and synthesis of biologically active compounds that can bind to DNA with a high affinity and specificity. There is an evidence that antitumour activity is due to the intercalation between the base pairs of DNA and interference with normal functioning of the enzyme topoisomerase II that is involved in the breaking and releasing of DNA strands [34]. Our previous study has demonstrated that the presence of oxime esters containing weak N–O bond showed photocleaving ability of DNA [34]. On the basis of introducing a fused aromatic ring to the oxime skeleton to result in higher antitumor and/or DNA photocleaving activities. The study of the reaction is greatly aided by the simple procedure, but this also implies that new variants must be unusually novel to be useful. We have been interested in developing the new anticancer drugs, particularly by radical species. Taking inspiration from the above and as a part of our continuing research on the synthesis and anticancer, antibacterial, DNA photocleavage and molecular docking studies of biologically active compounds [35,36]. Hence, the need to be replaced by newer drugs periodically. In this perspective, we proposed the synthesis and development of oxime esters unit targeting anticancer, antibacterial, DNA binding, DNA photocleavage and molecular docking. In continuation of our research, the main objective is to discover new anti-cancer agents.

2. MATERIALS AND METHODS

Materials and equipment

All the chemicals used in the present study are of AR grade. M/s Sigma-Aldrich, and Merck, USA and M/s S.D. Fine Chem. Pvt. Ltd, Mumbai, India. Calf thymus DNA (CT DNA) and supercoiled pUC19 DNA (cesium chloride purified) was obtained from Bangalore Genei (India). Agarose (low melt, 65°C, molecular biology grade for DNA gels), ethidium bromide, bromophenol blue, Tris(hydroxymethyl)aminomethane (Tris), sodium chloride, ethylene diamine tetraacetic acid disodium salt (EDTA-Na₂), sodium azide, were of molecular biology grade, obtained from Himedia (India).

Melting points were recorded on an open capillary tube with a Buchi melting point apparatus and are uncorrected. Elemental analyses were carried out using Perkin-Elmer 240C CHN-analyzer. IR spectra were recorded on a FT-IR infrared spectrophotometer. 1H- NMR spectra were obtained using a 300 MHz and 400 MHz on a Bruker spectrometer (chemical shifts in δ ppm). Mass spectra were recorded using a micro spray Q-TOF MS ES Mass spectrometer.

3. EXPERIMENTAL

General procedure for the preparation oxime esters:

Triethylamine (1.50 eq., 15 mmol, 2.10 mL) was added to a solution of oxime (1.00 eq., 10 mmol) in CH₂Cl₂ (15 mL) followed by a solution of acid chloride (1.05 eq., 10.5 mmol) in CH₂Cl₂ (15 mL), dropwise at room temperature. After 2 h of stirring water (20 mL) was added. The organic phase was separated, and the aqueous layer

was extracted with CH_2Cl_2 (3×10 mL). The combined organic phases were then washed with water (20 mL), dried over anhydrous $NaSO_4$, filtered and concentrated to give crude oxime ester which was purified by crystallization or flash chromatography.

- (*E*)-*Benzylideneamino-oxy-(phenyl)methanone* (*3a*). Yield 92%, m.p. 93–95 °C. IR (KBr): 1734 cm⁻¹. ¹H NMR (400 MHz, CDCl₃): δ 6.98-7.00 (d, *J*=8.0 Hz, 2H), 7.16-7.18 (d, *J*=8.0 Hz, 2H), 7.77-7.80 (d, *J*=8.0, 2H), 8.08-8.10 (d, *J*=8.0 Hz, 2H), 8.50 (s, 1H).
- (*E*)-*Benzylideneamino-oxy-*(*4-methoxyphenyl*)*methanone* (*3b*). Yield 94%. Colorless crystals, m.p. 97–99 °C. IR (KBr): 1732 cm⁻¹. ¹H NMR (400 MHz, CDCl₃): δ 3.80 (s, 3H), 6.97-6.99 (d, *J*=8.0 Hz, 2H), 7.16-7.18 (t, *J*=8.6 Hz, 2H), 7.80-7.82 (dd, *J*=8.0 Hz, 2H), 8.06-8.08 (d, *J*=8.0 Hz, 2H), 8.55 (s, 1H).
- (*E*)-4-Methyl-benzylideneamino-oxy-(4-methoxyphenyl)methanone (3c). Yield 90%. Colorless crystals, m.p. 128–130 °C. IR (KBr): 1729cm⁻¹. ¹H NMR (400 MHz, CDCl₃): δ 2.53 (s, 3H), 3.86 (s, 3H), 6.94-6.96 (d, *J*=8.0 Hz, 2H), 7.25-7.28 (d, *J*=8.0 Hz, 2H), 7.70-7.72 (d, *J*=8.0 Hz, 2H), 8.10-8.13 (d, *J*=8.0 Hz, 2H), 8.52(s, 1H).
- (*E*)-4-Methoxy-benzylideneamino-oxy-(4-methoxyphenyl)methanone (3d). Yield 90%. Colorless crystals, m.p. 147–149 °C. IR (KBr): 1733 cm⁻¹. ¹H NMR (400 MHz, CDCl₃): δ 3.84 (s, 3H), 3.90 (s, 3H), 6.96-6.98 (d, *J*=8.0 Hz, 2H), 7.08-7.11 (d, *J*=8.0 Hz, 2H), 7.78-7.80 (d, *J*=8.0 Hz, 2H), 8.08-8.10 (d, *J*=8.0 Hz, 2H), 8.48 (s, 1H). ¹³C NMR (75.5 MHz, CDCl₃): δ 55.6, 55.8, 113.5, 114.7 121.3, 122.8, 131.0, 131.6, 155.9, 162.6, 163.2, 163.5.
- (*E*)-4-Chloro-benzylideneamino-oxy-(4-methoxyphenyl)methanone (3*f*). Yield 88%. Colorless crystals, m.p. 151–152 °C. IR (KBr): 1732 cm⁻¹. ¹H NMR (400 MHz, CDCl₃): δ 3.86 (s, 3H), 6.95-6.98 (d, *J*=8.0 Hz, 2H), 7.41-7.44 (d, *J*=8.5 Hz, 2H), -7.72-7.74 (d, *J*=8.0 Hz, 2H), 8.06-8.08 (d, *J*=8.0 Hz, 2H); 8.53 (s, 1H). ¹³C NMR (75.5 MHz, CDCl₃): δ 55.3, 113.3, 121.4, 128.6, 129.4, 130.0, 131.5, 137.4, 155.6, 162.0, 163.0.
- (*E*)-4-Bromo-benzylideneamino-oxy-(4-methoxyphenyl)methanone (3g). Yield 75%. Colorless crystals, m.p. 162–164 °C. IR (KBr): 1733 cm⁻¹. ¹H NMR (400 MHz, CDCl₃): δ 3.90 (s, 3H), 6.96-6.98 (d, *J*=8.0 Hz, 2H), 7.56-7.58 (d, *J*=8.0Hz, 2H), 7.66-7.68 (d, *J*=8.0Hz, 2H), 8.08-8.10 (d, *J*=8.0 Hz, 2H), 8.56 (s, 1H).
- (*E*)-4-Fluoro-benzylideneamino-oxy-(4-methoxyphenyl)methanone (3i). Yield 90%, m.p. 116–118 °C. IR (KBr): 1730 cm⁻¹. ¹H NMR (400 MHz, CDCl₃): δ 3.89 (s, 3H), 6.95-6.99 (d, *J*=8.0 Hz, 2H), 7.15-7.18 (d, *J*=8.0 Hz, 2H), 7.80-7.82 (d, *J*=8.0, 5.4 Hz, 2H), 8.10-12 (d, *J*=0.0 Hz, 2H), 8.50 (s, 1H).
- (*E*)-*4*-(*Trifluoromethyl*)-*benzylideneamino-oxy*-(*4*-*methoxyphenyl*)*methanone* (*3j*). Yield 95%. Colorless crystals, m.p. 148–150 °C. IR (KBr): 1728 cm⁻¹. ¹H NMR (400 MHz, CDCl₃): δ 3.91 (s, 3H), 6.96-6.98 (d, *J*=8.0 Hz, 2H), 7.70-7.73 (d, *J*=8.0 Hz, 2H), 7.94-7.96 (d, *J*=8.0 Hz, 2H), 8.10- 8.13 (d, *J*=8.0 Hz, 2H), 8.62(s, 1H).
- (*E*)-4-Nitro-benzylideneamino-oxy-(4-methoxyphenyl)methanone (3k). Yield 85%. Yellowish crystals, m.p. 178–180 °C. IR (KBr): 1741 cm⁻¹. ¹H NMR (400 MHz, CDCl₃): δ 3.90 (s, 3H), 6.94-6.96 (d, *J*=8.0 Hz, 2H), 8.00-8.03 (d, *J*=8.1 Hz, 2H), 8.06-8.08 (d, *J*=8.0 Hz, 2H), 8.20-22 (d, *J*=8.0 Hz, 2H), 8.63 (s, 1H).

(*E*)-3,5-Dinitro-benzylideneamino-oxy-(4-methoxyphenyl)methanone (3l). Yield 95%. Colorless crystals, m.p. 183–185 °C. IR (KBr): 1748 cm⁻¹. ¹H NMR (400 MHz, CDCl₃): 3.92 (s, 3H), 6.78-6.81 (d, *J*=8.0 Hz, 2H), 6.94-6.97 (d, *J*=8.0 Hz, 2H), 7.64-7.67 (d, *J*=8.0 Hz, 2H), 8.06-8.08 (d, *J*=8.0 Hz, 2H), 8.55 (s, 1H).

4. RESULTS AND DISCUSSION

In our attempts to search for novel antitumor agents, we extended the interest to biocompatible oximes and synthesized series oxime derivatives with the aim of evaluating their diverse biological activity.

4.1. CHEMISTRY

Scheme 1: Synthetic route of Oxime esters. Reagents and conditions: (i) NH₂OH.HCl, Et₃N, EtOH, rt; (ii) RCOCl,Et₃N, CH₂Cl₂, 0°C.

As shown in Scheme 1 and Table 1, the treatment of substituted oximes with one molecules of aromatic acid chlorides in the presence of triethyl amine afforded the corresponding biocompatible oxime esters (3a–3l) in good yields (Scheme 1) [34]. These methodologies resulted in high yield of products with shorter reaction time for all the substrates (Table 1). The final products were well characterized using FT-IR, ¹H NMR spectra and mass spectrometry. In general, the compounds containing carbonyl group shows absorption in the region of 1600-1750 cm⁻¹. In all the compounds 3a–3l, strong band appeared in the double bond region at 1739-1752 cm⁻¹ which confirmed the formation of oxime ester (C=O). The presence of imino group (C=N) in the structure gives the band at 1641-1607 cm⁻¹. For the convenience, compound 3d has selected for the NMR spectral discussion, the two sets of signals appeared in the region 3.84 (s, 3H) and 3.90 (s, 3H), ppm with the presence of two methoxy functional groups. One singlet that appeared in the region at 8.48 ppm corresponds to the deshielded proton. In the ¹³C NMR spectrum of compound 3d, the aromatic C-atoms appeared in the region of 121.3-131.6 ppm. The imino carbon (C₄) and *O*-benzoyl carbonyl carbon appear in downfield region at 163.2 and 163.5 ppm, respectively. In the upfield region, methoxy group attached to aromatic carbon is observed at 55.6 and 55.8 ppm respectively.

4.2. BIOLOGICAL ACTIVITY

4.2.1. ANTIBACTERIAL ACTIVITY

All the synthesized oxime esters exhibited a wide range of *in vitro* antibacterial activity from higher concentration (10 µg/mL) against *Escherichia coli* and *Staphylococcus aureus* bacterial strains by disc diffusion method [37,38]. Discs measuring 6.25 mm in diameter were punched from Whatman no. 1 filter paper. Batches of 100 discs were dispensed to each screw capped bottles and sterilized by dry heat at 140 °C for an hour. The test compounds were prepared with different concentrations using dimethylsulphoxide. One milliliter containing 100 times the amount of chemical in each disc was added to each bottle, which contains 100 discs. The discs of each concentration were placed in triplicate in nutrient agar medium seeded with fresh bacteria separately. The incubation was carried out at 37 °C for 24 h. Ciprofloxacin was used as a standard drug. Solvent and growth controls were prepared and kept. Zones of inhibition and minimum inhibitory concentrations (MICs) were noted. The results of antibacterial studies are given in Table 2.

The investigation of antibacterial screening data revealed that all the tested compounds showed moderate to good bacterial inhibition. Compounds **3a-3l** are active at 10 mg/ml against *S. aureus* Compounds **3a, 3b, 3c, 3f, 3g, 3h, 3i, 3j, 3k, 3l**, are active at 10 mg/ml concentrations against *E. coli*. Compounds **3d** and **3e**, are inactive at 10 mg/ml concentrations against *E. coli*.

From the above observations, it is obvious that flouro (3i) substituted oxime esters recorded excellent activity; among the substituted oxime esters, chloro- and nitro-substituted oxime esters also registered good activity.

Table 1: Synthesis of oxime esters.

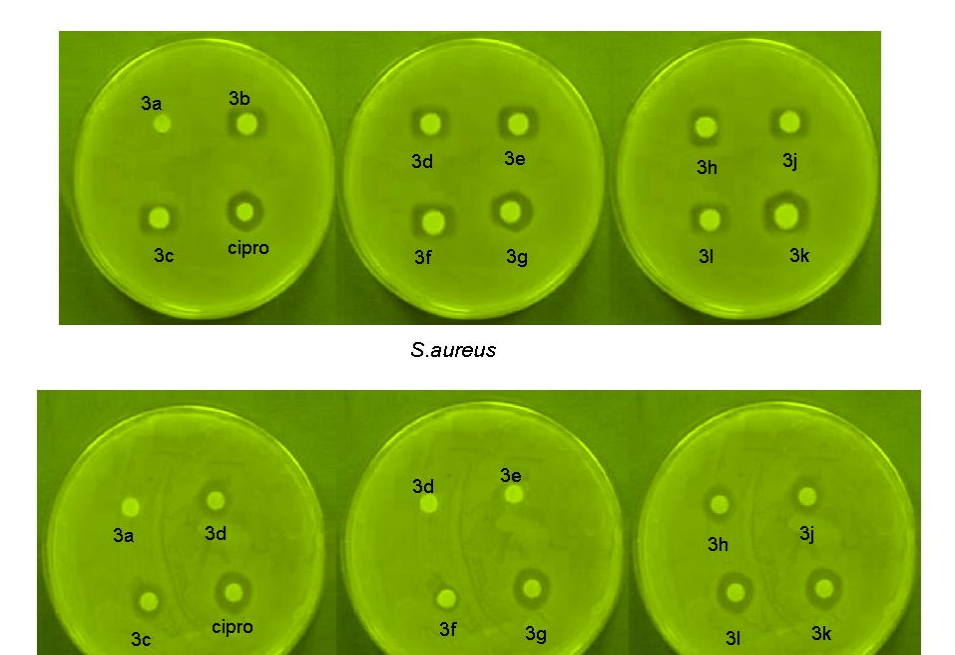
Entry	Product	MP	Yield (%)
3a		93-95	92
3b	H CMAC	97-99	94
3c	H O O O O O O O O O O O O O O O O O O O	128-130 °C	90
3d	Mac Obba	147-149 °C	90
3e	OMe H OMe	98-100 °C	92
3f	H OMe	150-152 °C	88
3g) OMe	162-164 °C	75

, relaille	11,10000 =		******
3h	Br H N O O	107-109 °C	70
3i	H OME	116-118 °C	90
3Ј	H CMa	148-150 °C	95
3k	N OMA	178-180 °C	85
31	O ₂ N O ₃ N O ₄ N O ₅ OMbe	183-185 °C	95

^a All the products were characterized by elemental analysis, ¹H NMR, ¹³C NMR and mass spectral data. ^bYields of isolated products

Table 2: *In-vitro* antimicrobial activity of **3(a-l)** derivatives.

	Zone of inhibition(mm)			
Compounds	S. aureus	E. coli		
	Concentration per well(200µg)			
3a	8	11		
3b	7.5	9		
3c	9	9		
3d	9.5	-		
3e	13	-		
3f	13	8		
3g	12	8.5		
3h	16	9		
3i	18	15		
3J	8.5	9		
3k	8.5	8.5		
31	9	9		
Ciprofloxacin(2.0µg/well)	21.2±0.44	21.2±0.83		



E.coli

Fig.2. Antibacterial activity of Biocompatible Oxime Esters.

4.2.2. ANTICANCER ACTIVITY

In literature, few reports were available of the anticancer activity of different heterocyles, by taking the The cytotoxic activity of the oxime esters against two human cancer cell lines such as MCF-7 (breast cancer) and HeLa cells (cervical carcinoma) were evaluated. For comparison, the corresponding standard drug doxorubicin used according to the literature procedures and their cytotoxicity evaluated [38,39]. Cultured cancer cells were treated with compounds with different concentrations for 48 h, and the percentage of cell growth inhibition was determined by MTT assay [38,39]. The GI₅₀ values are given in Table 3.

Considering the varied structure—activity relationships of different series of compounds, it cannot be inferred that the biological behaviour of a drug is determined by the influence of a single parameter or variable. Furthermore, in most cases, the presence or introduction of various functional groups in a compound does not allow to accurately explain the kind and intensity of its biological activity. However, and taking the necessary precautions, the information in Table 3 may allow us to make some general remarks on the structure and anticancer activity of the oxime esters. From Table 3, it is clear that anticancer activity of oxime esters increases accordingly on replacing hydrogen atom with oxygen and halogen atoms at 4-position of aromatic ring. Methoxy substitution on both aromatic ring analogues of oximes (3d) have more anticancer activity as compared to other derivatives. From the results, it was observed that, the compound (3e) was not so effective against MCF-7 cells. The oxime esters 3a, 3g and 3h were found to be inactive in both cell lines tested, except the 3d, 3d, 3i and 3j which is highly toxic to MCF-7 cells and HeLa cells compared with standard drug Doxorubicin (Table 3). This increase in activity is probably due to the presence of methoxy and fluorine at 4-position which is the most electronegative atom. Above

results show that electron-donating and electronegative groups are responsible for the anticancer activity of oxime esters provided these groups are at 4-position in ring-A and ring-B rather than any other position.

Table 3. Effect of oxime esters (OE) on proliferation of human cancer cell lines assessed by MTT assay. A fixed number of cells (1×10^4) grown in a 96-well culture plate were exposed to different concentrations of OE for 24 h followed by MTT addition and absorbance was recorded at 540 nm by ELISA reader. IC₅₀ value of after 24 h drug incubation with MCF-7 and HeLa cell lines by MTT assay. All values are expressed as mean \pm SEM.

Drugs	Conc.	% growth inhibition after 24 h incubation	
	(µg/mL)	MCF-7 cells	HeLa cells
	5	NA	NA
3a	10	NA	NA
	5	NA	NA
3b	10	42.16 ± 0.31	NA
	5	15.03 ± 0.11	16.00 ± 0.11
3c	10	38.57 ± 0.24	36.44 ± 1.00
	5	10.50 ± 0.66	11.09 ± 0.17
3d	10	20.78 ± 0.10	21.07 ± 0.10
	5	11.00 ± 0.50	10.88 ± 1.00
3e	10	20.11 ± 0.87	22.20 ± 1.04
	5	15.54 ± 0.05	16.08 ± 0.05
3f	10	42.87 ± 0.11	43.68 ± 0.15
	5	NA	NA
3 g	10	NA	NA
	5	NA	NA
3h	10	NA	NA
	5	12.03 ± 0.10	12.30 ± 1.04
3i	10	22.02 ± 0.10	23.42 ± 1.05
	5	12.57 ± 0.11	13.06 ± 1.04
3j	10	22.66 ± 0.10	23.10 ± 1.05
	5	17.33 ± 0.12	17.02 ± 1.04
3k	10	49.77 ± 0.12	47.24 ± 1.05
	5	19.22 ± 0.08	19.30 ± 1.04
31	10	36.95 ± 0.10	37.52 ± 1.05
Doxorubicin	5	14.03 ± 0.11	15.00 ± 0.11

4.2.3. DNA BINDING STUDIES.

Since DNA and genetic material contain all cellular information, the study of DNA interaction is a very important aspect at present. Interaction of small molecules with DNA has been investigated and it attracted more attention for the designing of more effective drugs which target to DNA. Classical and nonclassical intercalation and groove or electrostatic modes of binding have been studied by various interaction modes of drug-DNA [40–43]. Thus, studying the interactions of target compounds with DNA is important to get an indication about their anticancer impacts and imaginable mechanisms of action. In general, a compound and DNA formed covalent and noncovalent bonds. Through covalent bonding, a labile compound is switched by a nitrogen atom of the DNA base, such as N7 of guanine, in which the interactions like electrostatic, intercalation, and groove binding are conceivable in noncovalent binding [43,44]. Meanwhile, The change in the wavelength or absorption or both is characteristic of the

interactions and intercalative modes including strong stacking interactions between DNA base pairs and aromatic chromophores [43,44]. It is supposed that bathochromism means breakage of the secondary structure of DNA and hyperchromism involves covalent binding. Moreover, considerable red shifts revealed that the compounds were coordinated to DNA via N7 position of guanine [43-46]. On the other hand, no or slight shifts in UV spectra are indicative of an outside groove binding, generally with minor hyperchromicity [43-46].

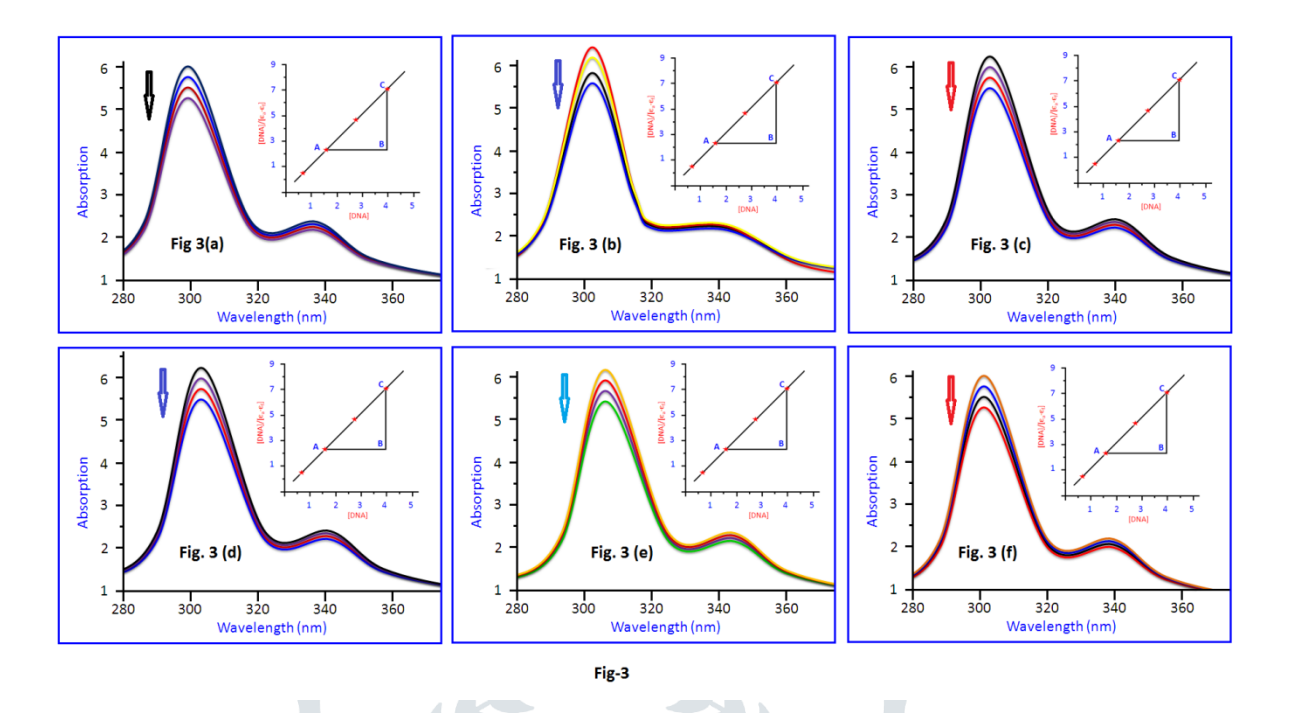


Fig.3. DNA binding studies of Biocompatible Oxime Esters (3a-3f). UV absorption spectra of (3a-3f) upon addition of calf thymus (ds) DNA. Concentration of control [DNA] = 0.5 μ M and we have increase the Concentration of [DNA] =10 μ M, 20 μ M and 30 μ M [---] respectively. Arrow shows the absorbance changing upon the increase of DNA concentration. The inner plot of [DNA]/(ϵ a- ϵ f) vs [DNA] for the titration of DNA with oxime ester.

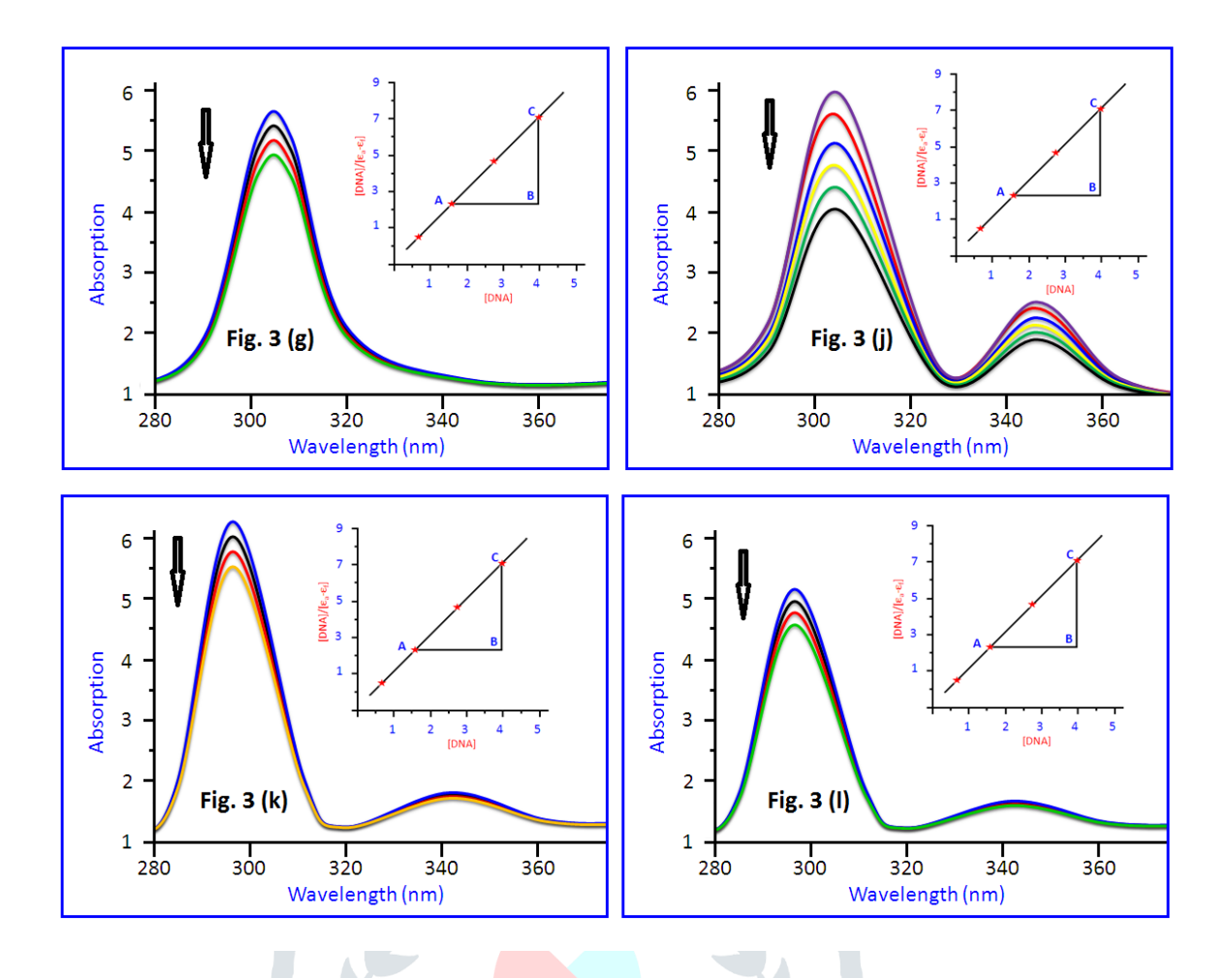


Fig.4. UV absorption spectra of (3g, 3j, 3k and 3l) upon addition of calf thymus (ds) DNA. Concentration of control [DNA] = 0.5 μM and we have increase the Concentration of [DNA] =10 μM, 20 μM and 30 μM [---] respectively. Arrow shows the absorbance changing upon the increase of DNA concentration. The inner plot of [DNA]/(εα-εf) vs [DNA] for the titration of DNA with oxime ester.

In this study, the absorption bands of the tested oxime esters (3a–31) are recorded in the absence and presence of CT-DNA. The DNA binding spectra for **3a**, **3b**, **3c**, **3d**, **3e**, **3f**, **3g**, **3j**, **3k** are shown in Fig. 3 and Fig. 4 respectively. The UV–vis spectral data for (3a–31) are summarized in Table 4. The association 3a to DNA in buffered solution was monitored by spectrophotometeric titrations. The effect of progressively increasing higher concentrations of DNA on the absorption spectra of oxime ester (**3j**) is shown in Fig. 3(j). The spectral change involved essentially a progressive red shift and hypochromicity, i.e., the interaction of oxime ester (**3j**) with DNA resulted in a strong decrease of the absorption intensity. The absorption of oxime ester (**3j**) in the peak was decreased by about 20.33% at 360 nm peak maximum along with a bathochromic shift of 3–5 nm. This hypochromism and bathochromic shift may be due to strong interaction between the electronic states of the interacalating chromophore and that of the DNA base pairs [40–43]. Such changes are obvious evidence of the

formation of DNA adducts. It is believed that these hypochromic shifts are probably due to the covalent and noncovalent bonds, which were observed in all target compounds [40].

4.2.4. DNA PHOTOCLEAVAGE STUDIES

Free radicals were mostly generated in various bio-oxidative processes that damage various body components such as fat and proteins and cause various harmful diseases such as cancer, hypertension, Parkinson's disease, and Alzheimer's disease. Therefore, to develop new therapeutic drugs to neutralize the effect or damage caused by free radicals is to achieve more attention [47,48]. The development of therapies which are selective for tumour tissues is one of the most important goals in anticancer research, within this framework photodynamic therapy (PDT) can be considered as a very promising approach [39].

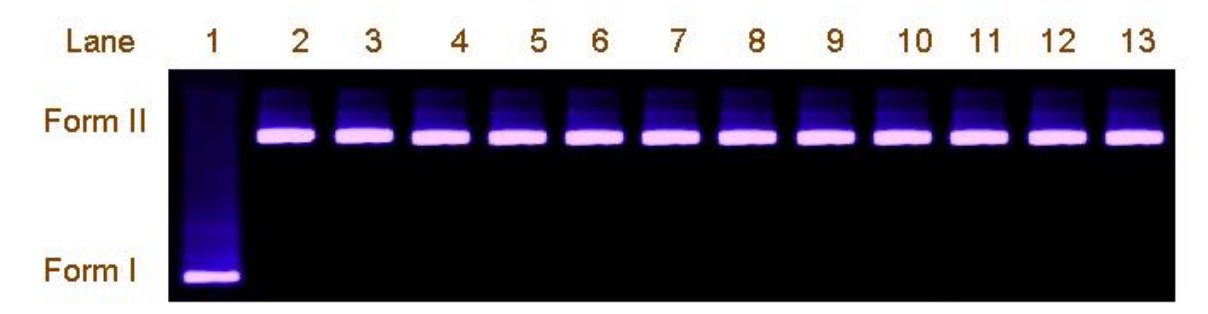


Fig. 5. pUC19 DNA photo cleavage by oxime esters (**3a-3l**) at 80μM concentration. The oxime esters (**3a-3l**) was irradiated with UV light at 365 nm. Lane; 1: control DNA (without compound), Lane 2 to Lane 13 with oxime esters.

The H abstraction from C-4' is the most important process in DNA cleavage. The gel Electrophoresis was an effective method for examining the DNA cleavage studies[39]. When circular plasmid DNA is subject to electrophoresis, relatively fast migration will be observed for the intact supercoil form (Form I). If scission occurs on one strand (nicking), the supercoil will relax to generate a slower-moving open circular form (Form II). If both strands are cleaved, a linear form (Form III) that migrates at rates between Form I and Form II will be generated [39]. From our previous results, the methoxy groups are highly reactive radicals, which abstracts hydrogen atoms efficiently at C-4' of 2-deoxyribose. It is of interest to note that methoxy group has been reported to bring about oxygen radical mediated DNA damage in the presence of photoirradiation. Therefore keeping in mind we have selected synthesis of alkoxy substituted oxime esters for nuceolytic activity [34].

The Fig. 5, shows gel electrophoresis separation of pUC19 DNA after incubation with different concentration of oxime esters and irradiated for 2h, in 1:9 DMSO/trisbuffer (20 μM, pH- 7.2) at 365 nm. No DNA cleavage was observed for the control in which oxime esters were absent (lane 1) (Fig. 5). The concentration depended DNA cleavage is also studied by selecting oxime esters like, **3a**, **3b**, **3d**, **3i**, **3j** and **3l**. With increasing concentration of these oxime esters (Fig. 6, lanes 2-7), the amount of Form I of pUC 19 DNA diminished gradually, whereas Form II increased (Fig. 6). At 40 μM concentration, the compound (**3d**) can promote only 18% conversion of DNA from Form I to II (Fig. 6). Whereas at 60 μM concentration, the compound (**3d**) can promote 45%

conversion of DNA from Form I to II (Fig. 6). But, the compound (**3d**) can almost promote 90% conversion of DNA from Form I to II at 80 μM concentration (Fig. 6).

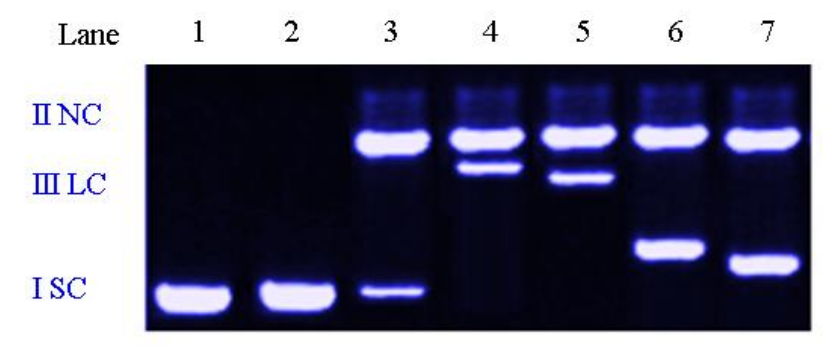


Fig. 6. Concetration-dependence of pUC19 DNA photocleavage by oxime ester. The oxime ester (3d) was irradiated with UV light at 365 nm. Lane-1: control DNA (without compound), Lane 2: DNA + (3d) 10μ M, Lane 3: DNA + (3d) 20μ M, Lane 4: DNA + (3d) 40μ M, Lane 5: DNA + (3d) 50μ M, Lane 6: DNA + (3d) 60μ M, Lane 7: DNA + (3d) 80μ M, respectively.

However, Fig. 7 shows the gel electrophoresis separation of pUC19 DNA at 80 μM concentration of oxime esters 3a-3l, the compound (3d) cleave efficiently, this is because of 3d has two methoxy substituent in structure. We have also observed the DNA separation by oxime esters at 80 μM concentration as shown in Fig. 7. Even at higher concentrations around 120 μM, compounds shows DNA cleavage activity, but around 140 μM concentration the compounds gets precipitated and there is no moment in the DNA. This reveals that, oxime esters nuclease is capable to accelerate the cleavage of plasmid DNA is purely concentration dependent.



Fig. 7. Light-induced cleavage of DNA by oxime esters at 365 nm. Supercoiled DNA runs at position I (SC), linear DNA at position III (LC) and nicked DNA at position II (NC). Lane; 1: control DNA (without compound), Lane; 2: 80μM (3a), Lane; 3: 80μM (3b), Lane; 4: 80μM (3c), Lane; 5: 80μM (3d), Lane; 6: 80μM (3e), Lane; 7: 80μM (3f), Lane; 8: 80μM (3g), Lane; 9: 80μM (3h) Lane; 10: 80μM (3i) Lane; 11: 80μM (3j) Lane; 12: 80μM (3k) Lane; 13: 80μM (3l).

4.2.5. MOLECULAR DOCKING STUDIES.

The DNA-drug and RNA-drug dockings of small organic compounds are generally less investigated. In particular, we did not find a docking scoring function for DNA-oxime ester molecular docking. The molecular dynamics of the DNA-drug complexes is central for drug design towards chemotherapy. Molecular dynamics has become the by

foremost well established, computational technique to investigate structure and function of bio-molecules and their respective complexes and interactions [49–51]. In this sense, it is of high relevance taking into account that, the previous non-covalent binding between drug and DNA has a strong influence on the subsequent photoreaction and therefore on their biological activity [39].

In order to rationalize the observed spectroscopic results and to get more insight into the intercalation modality, the oxime esters (3a–3l) were successively docked [39], within the DNA duplex of sequence d(CGCGAATTCGCG)₂ dodecamer (PDB ID: 1BNA) (Fig. 8) in order to predict the chosen binding site along with preferred orientation of the ligand inside the DNA minor groove. All synthesized oxime ester (3a–3l) derivatives were drawn in ChemSketch and structures were saved in .mol format. Afterwards the .mol format was used in Hyperchem-7, to adjust their fragments, followed by total energy minimization of ligands so that they can attain a stable conformation and the file was saved in .pdb format.

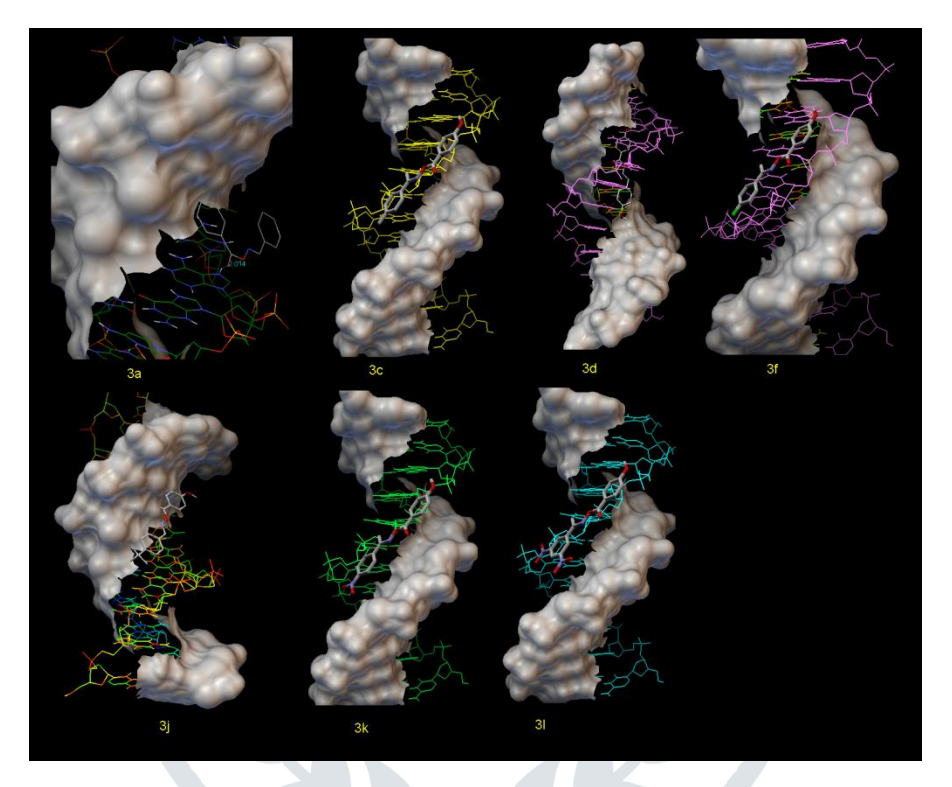


Fig. 8. View of the energy minimized docked poses of oxime esters (**3a-3l**) with DNA d(CGCGAATTCGCG)₂ (PDB ID: 1BNA).

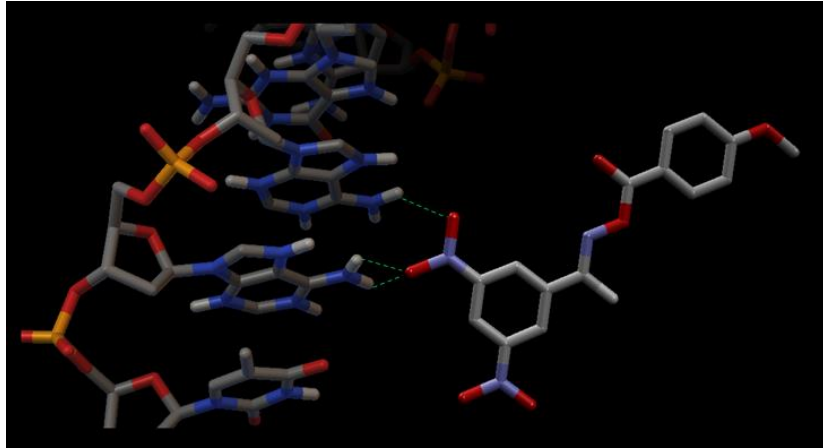


Fig. 8. Interaction of oxime esters (31) with DNA d(CGCGAATTCGCG)₂ (PDB ID: 1BNA).

Protein 3D structure of B-DNA was obtained from RCSB PDB (an information portal to biological macromolecular structures). The water molecules were removed from the file, and the protein was protonated in 3D to add polar hydrogen's. Binding pocket was identified using site finder, and the respective residues were selected. Docking parameters were set to default values and scoring algorithm, the docking runs were retained to 30 conformations per ligand. The docked protein structures were saved in .pdb format, and ligand's conformations were investigated one by one. Complexes with best conformations were selected on the basis of highest score, lowest binding energy and minimum RMSD values [39].

Table 4: Molecular Docking studies of oxime esters.

Products	Docking Energy	Inhibition constant	RMSD	DNA binding
	(Kcal/mol)	(M)		constant K _b
3a	-7.45	4.35 x 10 ⁻⁷	2.5	5.2 x 10 ⁴ M ⁻¹
3b	-25.60	3.84 x 10 ⁻¹⁶	2.5	$2.6 \times 10^4 \mathrm{M}^{-1}$
3c	-25.32	2.91 x 10 ⁻¹⁶	5.5	2.9 x 10 ⁴ M ⁻¹
3d	-25.89	2.96 x 10 ⁻⁷	3.4	5.8 x 10 ⁴ M ⁻¹
3e	-7.05	6.22 x 10 ⁻⁷	3.4	6.1 x 10 ⁴ M ⁻¹
3f	-7.47	6.76 x 10 ⁻⁷	3.8	5.7 x 10 ⁴ M ⁻¹
3g	-7.80	6.36 x 10 ⁻⁷	2.0	5.8 x 10 ⁴ M ⁻¹
3h	-7.32	7.55 x 10 ⁻¹⁶	2.0	6.2 x 10 ⁴ M ⁻¹
3i	-7.77	5.85 x 10 ⁻⁷	2.5	5.5 x 10 ⁴ M ⁻¹
3j	-24.07	2.41 x 10 ⁻¹⁶	2.0	2.5 x 10 ⁴ M ⁻¹
3k	-7.39	6.33 x 10 ⁻⁷	2.5	5.6 x 10 ⁴ M ⁻¹
31	-8.22	6.10 x 10 ⁻⁷	2.5	5.5 x 10 ⁴ M ⁻¹

Molecular docking was carried out between rigid receptor protein and the flexible oxime esters. Table 4 shows the details of the docking results including RMSD and binding energy values of protein–ligand complexes. The oxime esters (**3b**, **3c**, **3d** and **3j**) bind strongly to B-DNA as inferred by their minimum binding energy values, that is, -25.60, -25.32, -25.89 and 24.07 kcal/mol, respectively as shown in Table 4 (Fig. 8). Interaction of DNA base pairs with compound 31 was showed in Fig. 9. Docked compounds were analysed in terms of hydrogen bonding, energy, noncovalent, and hydrophobic interaction between compounds and DNA. The docked results clearly explained that there is strong interaction between the compounds and 1BNA.

CONCLUSION

In conclusion, we have synthesized biocompatible oxime esters and evaluated their biological and nucleolytic activity. The synthesized oxime esters were demonstrated as versatile synthons for the antibacterial, anticancer, DNA binding and DNA Photoclevage studies. Few compounds showed good bacterial inhibition almost equivalent to standard drug. It is concluded from the results that substituents on the oxime esters skeleton are responsible for the enhancement of the antibacterial activity. It can further be concluded that the percentage inhibition of anticancer activity increases as the electronegativity of the aromatic ring increases. Upon photoirradiation, the iminyl and carboxy radicals resulting from N-O bond homolysis of oximes are highly reactive radicals, which abstracts hydrogen atoms efficiently at C-4' of 2-deoxyribose of B DNA. The presences of methoxy substituents in the aryl group of oxime 3d responsible for spontaneous photolysis to radicals might be more efficient compare to the other oxime esters to cleave DNA. Results obtained from our present work would be very useful to understand the radical photoinduced DNA cleavage. The initial in-vitro biological activity and docking studies showed that the oxime ester scaffold had little effect on the antitumor activities, while variations in substitutions of the aryl moieties had a significant impact on the activities and alkoxy substitution produced the best potency. Further studies will be carried out in near future.

FUNDING

Author P. J. B. thank Dr. D. S. Kothari post doctoral fellowship, UGC, INDIA, for financial support.

CONFLICT OF INTEREST

Author P. J. B. thank Dr. D. S. Kothari post doctoral fellowship, UGC, INDIA, for financial support.

ACKNOWLEDGEMENTS

Author P. J. B. thank Dr. D. S. Kothari post doctoral fellowship, UGC, INDIA, for financial support and Department of Organic Chemistry, Indian Institute of Science for giving an oppartunity to work.

REFERENCES

- 1. Wilson, W. D. In Nucleic Acids in Chemistry and Biology, ed. Blackburn G. M.; Gait, M. J. IRL Press., Oxford, **1989**, ch. 8.
- 2. Neidle, S.; Jenkins, T. C. Molecular Design and Modeling., Part B, **1991**, 203, 433.

- 3. Sartorius, J.; Schneider, H-J. Intercalation mechanisms with ds-DNA: binding modes and energy contributions with benzene, naphthalene, quinoline and indole derivatives including some antimalarials, J. Chem. Soc., Perkin Trans. 2, **1997**, 2319-2327.
- 4. Ravikumar Naik, T. R.; Bhojya Naik, H. S.; Prakash Naik, H. R.; Bindu, P. J.; Harish, B. G.; Krishna, V. Synthesis, DNA binding, docking and photoclevage studies of novel benzo[b][1,8]naphthyridines, Med. Chem. **2009**, *5*, 411-418. doi: 10.2174/157340609789117804.
- 5. Bindu, P. J.; Ravikumar Naik, T. R.; Mahadevan, K. M.; Krishnamurthy, G. Synthesis, DNA photocleavage, molecular docking and anticancer studies of 2-methyl-1,2,3,4-tetrahydroquinolines, Chem. Bio. Lett., **2019**, *6*, 8-13.
- Zhou, X.-Q.; D.-Y. Y. Li,; Nie, Z-Y.; Li, Z.-J.; Gu, W. Copper complexes based on chiral Schiff-base ligands: DNA/BSA binding ability, DNA cleavage activity, cytotoxicity and mechanism of apoptosis, Eur. J. Med. Chem., 2016, 114, 244–256.
- 7. Inamdar, P. R.; Chauhan, R.; Abraham. J.; Sheela, A. DNA interaction and cytotoxic activity of copper complex based on tridentate hydrazone derived ligand and nitrogen donor heterocycle, Inorg. Chem. Commun., **2016**, *67*, *67*–*71*.
- 8. Shokohi-Pour, Z.; Chiniforoshan, H.; Momtazi-Borojeni, A. A.; Notash, B. A novel Schiff base derived from the gabapentin drug and copper (II) complex: Synthesis, characterization, interaction with DNA/protein and cytotoxic activity, J. Photochem. Photobiol., B, **2016**, *162*, 34–44.
- 9. Pradhan, R.; Banik, M.; Cordes, D. B.; Slawin, A. M. Z.; Saha, N. C. Synthesis, characterization, X-ray crystallography and DNA binding activities of Co (III) and Cu (II) complexes with a pyrimidine-based Schiff base ligand, Inorg. Chim. Acta, **2016**, *442*, 70–80.
- 10. Abdel-Rahman, L. H.; Abu-Dief, A. M.; Ismael, M.; Mohamed, M. A. A.; Hashem, N. A. Synthesis, structure elucidation, biological screening, molecular modeling and DNA binding of some Cu (II) chelates incorporating imines derived from amino acids, J. Mol. Struct., **2016**, *1103*, 232–244.
- 11. Hussain, A.; Lahiri, D.; Ameerunisha, B. M. S.; Saha, S.; Majumdar, R.; Dighe, R. R.; Chakravarty, A. R. Photocytotoxic Lanthanum(III) and Gadolinium(III) Complexes of Phenanthroline Bases Showing Light-Induced DNA Cleavage Activity, Inorg. Chem., 2010, 49, 4036–4045.
- 12. Lahiri, D.; Roy, S.; Saha, S.; Majumdar, R.; Dighe, R. R.; Chakravarty, A. R. Anaerobic DNA cleavage activity in red light and photocytotoxicity of (pyridine-2-thiol)cobalt(iii) complexes of phenanthroline bases, Dalton Trans., **2010**, *39*, 1807–1816.
- 13. Detty, M. R.; Gibson, S. L.; Wagner, S. J. Current clinical and preclinical photosensitizers for use in photodynamic therapy, J. Med. Chem., **2004**, *47*, 3897–3915.
- 14. Henderson, B. W.; Busch, T. M.; Vaughan, L. A.; Frawley, N. P.; Babich, D.; Sosa, T. A.; Zollo, J. D.; Dee, A. S.; Cooper, M. T.; Bellnier, D. A.; Greco, W. R.; Oseroff, A. R. Photofrin photodynamic therapy can significantly deplete or preserve oxygenation in human basal cell carcinomas during treatment, depending on fluence rate, Cancer Res., **2000**, *60*, 525–529.

- 15. DeRosa, M. C.; Crutchley, R. J. Coord. Photosensitized singlet oxygen and its applications, Chem. Rev., **2002**, *233*, 351–357.
- 16. Szacilowski, K.; Macyk, W.; Drzewiecka-Matuszek, A.; Brindell, M.; Stochel, G. Bioinorganic photochemistry: frontiers and mechanisms, Chem. Rev., 2005, 105, 2647–2694.
- 17. Basak, A.; Mandal, S.; Bag, S. S. Chelation-Controlled Bergman Cyclization: Synthesis and Reactivity of Enediynyl Ligands, Chem. Rev., **2003**, *103*, 4077–4094.
- 18. Sharma, S.; Kaur, C.; Budhiraja, A.; Gupta, M.; Bedi, P. M. S. Chalcone based azacarboline analogues as novel antitubulin agents: Design, synthesis, biological evaluation and molecular modelling. Euro. J. Med. Chem., **2014**, *85*, 648-660.
- 19. Trott, O.; Olson, A. J. AutoDock Vina: improving the speed and accuracy of docking with a new scoring function, efficient optimization, and multithreading. J. Comput. Chem., **2010**, *31*, 455-461.
- 20. Bax, B. D.; Chan, P. F.; Eggleston, D. S.; Fosberry, A.; Gentry, D. R. Type IIA topoisomerase inhibition by a new class of antibacterial agents. Nature., **2010**, *466*, 935-940.
- 21. Huang, S.; Li, R.; Connolly, P. J.; Xu, G.; Gaul, M. D.; Emanuel, S. L.; LaMontagne, K. R.; Greenberger, L. M. Synthesis and biological study of 4-aminopyrimidine-5-carboxaldehyde oximes as antiproliferative VEGFR-2 inhibitors, Bioorg. Med. Chem. Lett., 2006, 16, 6063-66. doi: 10.1016/j.bmcl.2006.08.107.
- 22. Chen, Y.-L.; Chen, I.-L.; Lu, C.-M.; Tzeng, C-C.; Tsao, L.-T.; Wang, J.-P. Synthesis and anti-inflammatory evaluation of 4-anilinofuro[2,3-b]quinoline and 4-phenoxyfuro[2,3-b]quinoline derivatives. Part 3, Bioorg. Med. Chem. Lett., **2004**, *12*, 387-392, doi: **10**.1016/j.bmc.2003.10.051.
- 23. Chen, Y.-L.; Lu, C.-M.; Chen, I.-L.; Tsao, L.-T.; Wang, J.-P. Synthesis and antiinflammatory evaluation of 9-anilinoacridine and 9-phenoxyacridine derivatives, J. Med. Chem., **2002**, *45*, 4689-4694. doi: 10.1021/jm020102v.
- 24. Chen, Y.-L.; Chung, C.-H.; Chen, I.-L.; Chen, P.-H.; Jeng, H.-Y. Synthesis and cytotoxic activity evaluation of indolo-, pyrrolo-, and benzofuro-quinolin-2(1H)-ones and 6-anilinoindoloquinoline derivatives, Bioorg. Med. Chem., **2002**, *10*, 2705-2712. doi: 10.1016/s0968-0896(02)00111-6.
- 25. Hong, C. Y.; Kirn, Y. K.; Chang, J. H.; Kim, S. H.; Choi, H.; Nam, D. H.; Kim, Y. Z.; Kwak, J. H. Novel fluoroquinolone antibacterial agents containing oxime-substituted (aminomethyl)pyrrolidines: synthesis and antibacterial activity of 7-(4-(aminomethyl)-3-(methoxyimino)pyrrolidin-1-yl)-1-cyclopropyl-6-fluoro-4-oxo-1,4-dihydro[1,8]naphthyridine-3-carboxylic acid (LB20304), J. Med. Chem., **1997**, *40*, 3584-3593. doi: 10.1021/jm970202e.
- 26. Dallavalle, S.; Ferrari, A.; Biosotti, B.; Merlini, L.; Pence, S.; Gallo, G.; Marzi, M.; Tinti, M. O.; Martinelli, R.; Pisano, C.; Carminati, P.; Carenini, N.; Beretta, G.; Perego, P.; De Cesare, A.; Pratesi, G.; Zunino, F. Novel 7-oxyiminomethyl derivatives of camptothecin with potent in vitro and in vivo antitumor activity, J. Med. Chem., 2001, 44, 3264-74. doi: 10.1021/jm0108092.

- 27. Heinisch, G.; Holzer, W.; Kunz, F.; Langer, T.; Lukavsky, P.; Pechlaner, C.; Weissenberger, H. On the bioisosteric potential of diazines: diazine analogues of the combined thromboxane A2 receptor antagonist and synthetase inhibitor Ridogrel, J. Med. Chem., **1996**, *39*, 4058-64. doi: 10.1021/jm960341g.
- 28. Abele, E.; Abele, R. Oximes of Nucleosides and Related Compounds: Synthesis, Reactions and Biological Activity, Curr. Org. Synth., **2018**, *15*, 650–665.
- 29. Abele, E.; Abele, R. Recent Advances in the Synthesis of Heterocycles from Oximes, Curr. Org. Synth., **2014**, *11*, 403–428.
- 30. Brokenshire, J. L.; Roberts, J. R.; Ingold, K. U. Kinetic applications of electron paramagnetic resonance spectroscopy. VII. Self-reactions of iminoxy radicals. J. Am. Chem. Soc., **1972**, *94*, 7040–7049.
- 31. Eisenhauer, B.M.; Wang, M.; Brown, R.E.; Labaziewicz, H.; Ngo, M.; Kettinger, K.W.; Mendenhall, G.D. Spectral and kinetic measurements on a series of persistent iminoxyl radicals. J. Phys. Org. Chem., **1997**, *10*, 737–746.
- 32. Walton, J. C. Functionalised Oximes: Emergent Precursors for Carbon-, Nitrogen- and Oxygen-Centred Radicals, Molecules., **2016**, *21*, 63; doi:10.3390/molecules21010063.
- 33. Schepetkin, I. A.; Plotnikov, M. B.; Khlebnikov, A. I.; Plotnikova, T. M.; Quinn, M. T. Oximes: Novel Therapeutics with Anticancer and Anti-Inflammatory Potential, Biomolecules., **2021**, *11*, 777. https://doi.org/10.3390/biom11060777.
- 34. Bindu, P. J.; Mahadevan, K. M.; Satyanarayan, N. D.; Ravikumar Naik, T. R. Synthesis and DNA cleavage studies of novel quinoline oxime esters, Bioorg. Med. Chem. Lett., **2012**, 22, 898-900. doi: 10.1016/j.bmcl.2011.12.037.
- 35. Bindu, P. J.; Mahadevan, K. M.; Ravikumar Naik, T. R. An efficient one-pot synthesis and photoinduced DNA cleavage studies of 2-chloro-3-(5-aryl-4,5-dihydroisoxazol-3-yl)quinolines, Bioorg. Med. Chem. Lett., **2012**, *22*(2), 6095-8. doi: 10.1016/j.bmcl.2012.08.034.
- 36. Bindu, P. J.; Mahadevan, K. M.; Ravikumar Naik, T. R. Sm(III)nitrate-catalyzed one-pot synthesis of furano[3,2c]-1,2,3,4-tetrahydroquinolines and DNA photocleavage studies, J. Mol. Struct., **2012**, *1020*, 142-147.
- 37. Ravikumar Naik, T. R.; Shivashankar, S. A.; Bindu, P. J. Microwave-assisted synthesis of copper nanoparticles: influence of copper nanoparticles morphology on the antimicrobial activity, J. Mat. NanoSci., **2020**, *7*(2), 62-67.
- 38. Mahanthesha□, G.; Suresh, T.; Ravikumar Naik, T. R. Synthesis, docking and biological evaluation of 3-(3-chlorobenzoyl)-n-phenylindolizine-1-carboxamide derivatives as anti-tuberculosis, anticancer, anti-inflammatory and antibacterial agents, Rasayan J. Chem., **2022**, *15*(1), 155-161.
- 39. Ravikumar Naik, T. R. Therapeutic significance of 1,4-Dihydropyridine compounds as potential anticancer agents, Organic synthesis, Intech Open, publications., **2020**. DOI: 10.5772/intechopen.89860.

- 40. Bindu, P. J.; Ravikumar Naik, T. R.; Mahadevan, K. M. Synthesis, DNA binding, docking and photocleavage studies of 2-chloro-3-quinolinyl-3-phenylpropen-2-ones, Med.Chem.Comm, **2014**, *5*, 1708-1717.
- 41. Sangeetha Gowda, K. R.; Bhojya Naik, H. S.; Vinay Kumar, B.; Sudhamani, C. N.; Sudeep, H. V.; Ravikumar Naik, T. R.; Krishnamurthy. G. Synthesis, antimicrobial, DNA-binding and photonuclease studies of Cobalt(III) and Nickel(II) Schiff base complexes, Spectrochim. Acta A: Mol. Biomol. Spectrosc., 2013,105, 229–237.
- 42. Pradeepa, S. M.; Bhojya Naik, H. S.; Vinay Kumar, B.; Indira Priyadarsini, K.; Atanu Barik, Ravikumar Naik. T. R. Cobalt(II), Nickel(II) and Copper(II) complexes of a tetradentate Schiff base as photosensitizers: Quantum yield of 1O2 generation and its promising role in anti-tumor activity, Spectrochim. Acta A: Mol. Biomol. Spectrosc., **2013**,*101*, 132–139.
- 43. Ali, I.; Haque, A.; Saleem, K.; Hsieh, M.-F. Curcumin-I Knoevenagel's condensates and their Schiff's bases as anticancer agents: Synthesis, pharmacological and simulation studies. Bioorg. Med. Chem., **2013**, *21*, 3808–3820, DOI: 10.1016/j.bmc.2013.04.018.
- 44. Shahabadi, N.; Kashanian, S.; Mahdavi, M.; Sourinejad, N. DNA interaction and DNA cleavage studies of a new platinum (II) complex containing aliphatic and aromatic dinitrogen ligands. Bioinorg. Chem. Appl., **2011**, *2011*, 525794 DOI: 10.1155/2011/525794.
- 45. Roviello, G. N.; Vicidomini, C.; Di Gaetano, S.; Capasso, D.; Musumeci, D.; Roviello, V. Solid phase synthesis and RNA-binding activity of an arginine-containing nucleopeptide. RSC Adv., **2016**, *6*, 14140–14148, DOI: 10.1039/C5RA25809J.
- 46. Erkkila, K. E.; Odom, D. T.; Barton, J. K. Recognition and reaction of metallo intercalators with DNA. Chem. Rev., 1999, 99, 2777–2796, DOI: 10.1021/cr9804341.
- 47. Kamatchi, T. S.; Chitrapriya, N.; Ashok Kumar, S. L. The effect of incorporating carboxylic acid functionalities into 2,2'-bipyridine on the biological activity of the complexes formed: synthesis, structure, DNA/protein interaction, antioxidant activity and cytotoxicity, RSC Adv., 2017, 17, 16428–16443.
- 48. Barton, J. K.; Danishefsky, A.; Goldberg, J. Tris(phenanthroline)ruthenium(II): stereoselectivity in binding to DNA," J. Am. Chem. Soc., **1984**, *106*, 2172–2176.
- Abdel-Sayed, M. A.; Bayomi, S. M.; El-Sherbeny, M. A.; Abdel-Aziz, N. I.; ElTahir, K. E. H.; Shehatou, G. S. G.; Abdel-Aziz, A. A.-M. Synthesis, anti-inflammatory, analgesic, COX-1/2 inhibition activities and molecular docking study of pyrazoline derivatives, Bioorg. Med. Chem., 2016, 24, 2032–2042.
- 50. Tu, Y.; OuYang, Y.; Xu, S.; Li, Y. Z. G.; Sun, C.; Zheng, P.; Zhu, W. Design, synthesis, and docking studies of afatinib analogs bearing cinnamamide moiety as potent EGFR inhibitors, Bioorg. Med. Chem., **2016**, *24*, 1495–1503.
- 51. Mabkhot, Y. N.; Al-Har, M. S.; Barakat, A.; Aldawsari, F. D.; Aldalbahi, A.; Ul-Haq, Z. Synthesis, antimicrobial and molecular docking studies of quinazolin-4(3H)-one derivatives, Molecules., **2014**, *19*, 8725-8739.